

# Can a Pseudo Periodic Orbit Avoid a Catastrophic Transition?

Tetsushi Ueta

*Center for Administration of Information Technology, Tokushima University,  
2-1, Minami-Josanjima, Tokushima, 770-8506, Japan  
ueta@tokushima-u.ac.jp*

Daisuke Ito

*Department of Electronic Systems Engineering, School of Engineering, University of Shiga Prefecture  
2500, Hassaka-cho, Hikone-City, Shiga 522-8533 Japan*

Kazuyuki Aihara<sup>\*</sup>

*Institute of Industrial Science, The University of Tokyo,  
Tokyo 153-8505, Japan  
aihara@sat.t.u-tokyo.ac.jp*

Received (to be inserted by publisher)

We propose a resilient control scheme to avoid catastrophic transitions associated with saddle-node bifurcations of periodic solutions. The conventional feedback control schemes related to controlling chaos can stabilize unstable periodic orbits embedded in strange attractors or suppress bifurcations such as period-doubling and Neimark-Sacker bifurcations whose periodic orbits are kept existing through bifurcation processes. However, it is impossible to apply these methods directly to a saddle-node bifurcation since the corresponding periodic orbit disappears after such a bifurcation. In this paper, we define a pseudo periodic orbit which can be obtained using transient behavior right after the saddle-node bifurcation, and utilize it as reference data to compose a control input. We consider a pseudo periodic orbit at a saddle-node bifurcation in the Duffing equations as an example, and show its temporary attraction. Then we demonstrate suppression control of this bifurcation, and show robustness of the control. As a laboratory experiment, a saddle-node bifurcation of limit cycles in the BVP oscillator is explored. A control input generated by a pseudo periodic orbit can restore a stable limit cycle which disappeared after the saddle-node bifurcation.

*Keywords:* catastrophic transition, saddle-node bifurcation, unstable periodic orbit, pseudo periodic orbit, suppression of bifurcation

## 1. Introduction

Since catastrophic transitions at tipping points are widely observed in complex systems of the real world, detection of early warning signals for such transitions has been intensively studied [Scheffer *et al.*, 2009; Scheffer, 2009; Chen *et al.*, 2012]. But what can we do beyond the tipping points? This is the problem we

---

<sup>\*</sup>Author for correspondence

consider in this paper. In particular, we propose a resilient control scheme available beyond tipping points especially associated with saddle-node bifurcations in order to avoid catastrophic transitions.

Suppose that a dynamical system is represented by the following differential equation:

$$\frac{d\mathbf{x}}{dt} = \mathbf{f}(t, \mathbf{x}, \boldsymbol{\lambda}), \quad (1)$$

where  $\mathbf{x} \in \mathbf{R}^n$  is the state,  $t$  is the continuous time, and  $\mathbf{f} : \mathbf{R}^n \times \mathbf{R} \rightarrow \mathbf{R}^n$  is a  $C^\infty$ -class nonlinear map. By varying the parameters  $\boldsymbol{\lambda} \in \mathbf{R}^k$ , the structure of the flow (a family of solutions) may qualitatively change through a bifurcation. If an equilibrium point  $\mathbf{x}^*$  satisfying  $\mathbf{f}(\mathbf{x}^*) = \mathbf{0}$  encounters a bifurcation, basically the stability of the point changes. Roughly speaking, classic control problems almost focus on how to change the unstable equilibrium into a stable one, or how to retain the equilibrium stable against parameters variation, disturbances, and noise.

A nonlinear system sometimes produces periodic motion. A limit cycle of an autonomous system is generated, for example, by a supercritical Hopf bifurcation of the equilibrium, and represents oscillatory behavior. By changing the parameter values, the limit cycle also meets bifurcations. When a transversal section is provided as the Poincaré section, the dynamical behavior of the limit cycle is represented by a map  $T$  called the Poincaré map on the section. For periodically forced systems, the Poincaré map is obtained by a stroboscopic map observed with a constant time interval synchronized with the forcing period. A fixed point  $\mathbf{x}^*$  of  $T$  satisfies  $\mathbf{x}^* = T(\mathbf{x}^*)$ , and corresponds to a periodic solution  $\mathbf{x}(t)$ . The roots of the characteristic equation with respect to the Jacobian matrix of  $T$  at this fixed point are called the Floquet multipliers, and they determine the stability of the periodic solution, e.g., when one of them takes  $-1$ , the objective limit cycle becomes unstable, and a new 2-periodic solution appears around the periodic solution through a period-doubling bifurcation. When a couple of them take complex conjugates and its radius is unity, the objective periodic solution also becomes unstable, and a quasi-periodic solution emerges around the unstabilized cycle through a Neimark-Sacker bifurcation. Although we describe bifurcations of autonomous systems in the next section, similar bifurcations appear in non-autonomous systems as well.

## 2. Stabilizing unstable periodic orbits

Given a strange attractor, countably infinite unstable periodic orbits (UPOs) are embedded inside. For example, a period-doubling cascade, which is known as a route to chaos, leaves a lot of  $2^m$ -periodic UPOs at the accumulating point of the successive period-doubling bifurcations, where  $m = 0, 1, \dots, \infty$ . Ott, Grebogi and Yorke [Ott *et al.*, 1990] proposed an epoch-making paradigm called controlling chaos, or the OGY method; namely they demonstrated that a tiny control input can stabilize a saddle-type UPO. By taking the Poincaré mapping, the recurrence property of chaos makes the orbit to visit a neighborhood of an unstable periodic point (UPP) corresponding to the target UPO, and a stable manifold of that point leads the controlled orbit to UPO effectively.

On the other hand, Pyragas proposed another important concept of controlling chaos, called the delayed feedback control (DFC) [Pyragas, 1992] where a continuous-time control input based on difference between the current state and the delayed state is applied. The controlled system also has the ability to seek a UPO autonomously from an appropriate initial condition. Unlike the OGY control, while it does not require detailed information about the location of the target UPO beforehand, we cannot predict which UPO will be stabilized. The DFC controller for electrical circuits [Celka, 1994] can be realized with an analog delay element [Pyragas, 2006] although its period should be determined by a preliminary analysis or by trial and error. Theoretical issues on stability analysis and design of a suitable gain are not simple since the controlled system becomes an infinite-dimensional dynamical system. Chen and Dong [Chen & Dong, 1993] proposed a similar method, but the target UPO is not embedded in a chaotic attractor. It is theoretically illustrated that the controlled orbit is autonomously conveyed into a target UPO which is outside the chaotic attractor. The control schemes in terms of stabilizing UPO can be recognized as a linear control problem near the target UPP. Chen *et al.* also compiled works on “bifurcation control” [Chen *et al.*, 2003] such as changing parameter values of an exiting bifurcation point, stabilizing a bifurcated solution or branch, and delaying the appearance of the bifurcation. The approaches introduced in the literature are basically to change the system design.

A saddle-node (SN) bifurcation is a typical codim-1 local bifurcation, and exhibits coalesce and disappearance of two equilibria. This phenomenon is frequently used for explanation on catastrophe, hysteresis, and bistability. For periodic solutions, by taking the Poincaré mapping, a couple of node-type and saddle-type fixed points collide and disappear. Arnold's tongue is edged by this bifurcation that is trackable since one of the multipliers is equal to unity. In physical systems, the SN bifurcation is sometimes recognized as a sudden shift of the behavior arising from the parameter variation. Many catastrophe, hysteresis, and bistable models are explained qualitatively by existence of the SN bifurcations.

Suppressing local bifurcations has been intensively discussed for a decade from viewpoints of both control engineering applications and bifurcation control [Ogorzalek , 1993; Chen , 1999]. The former is an extension of controlling chaos when we locate a specific UPO in the given strange attractor. For discrete-time systems, OGY-type control input is given by

$$\mathbf{u}(k) = K(\mathbf{x}(k) - \mathbf{x}^*), \quad (2)$$

where  $k \in \mathbf{Z}$  is an integer, and  $\mathbf{x}^*$  is a target UPO [Romeiras *et al.* , 1992].

Let  $\mathbf{x}^*(t) \in \mathbf{R}^n$  with time  $t \in \mathbf{R}$  be a UPO of a continuous-time system. Then the control input of the delayed feedback control, the external force control (EFC), or the linear state feedback control is given by

$$\mathbf{u}(t) = K(\mathbf{x}(t) - \mathbf{x}^*(t)). \quad (3)$$

Note that both control inputs Eqs. (2) and (3) refer to certain information  $\mathbf{x}^*$  or  $\mathbf{x}^*(t)$  which really exists in the system itself. This fact induces an accompanied problems; how to find such reference information. To compute sufficient information about UPP or UPO, analytical methods [Diakonou *et al.*, 1998] or numerical methods with heuristic strategies [Ueta *et al.*, 2000] are required. The DFC utilizes a delayed data  $\mathbf{x}(t - \tau)$  as a reference  $\mathbf{x}^*(t)$ , and has ability to seek a UPO autonomously. Also note that these feedback systems can produce the periodic motion without a stationary parameter deviation as  $\mathbf{u}(t) \rightarrow \mathbf{0}$ . In other words, the system design is unchanged.

For period-doubling and Neimark-Sacker bifurcations, the objective periodic point corresponding to the periodic solution survives through a bifurcation process although its stability is changed, i.e., the point still exists after the bifurcation. Thereby the location or time series data of this point can be reference information  $\mathbf{x}^*$  or  $\mathbf{x}^*(t)$  for Eq. (2) or (3). With appropriate choice of the feedback gain, this target orbit may be stabilized. In addition, the bifurcation can be suppressed if the reference information is given adaptively as the parameter changes [Christini & Collins , 1996].

However, how about cases of SN bifurcations? As mentioned above, a couple of points vanish according to a parameter variation. Therefore it is impossible to suppress SN bifurcations with the conventional frameworks with Eqs. (2) and (3) as reference information does not exist any more after the bifurcations. Dependable clues passed off. Note also that SN bifurcations occur not only for a stable node and a one-dimensionally unstable saddle but also  $j$  and  $j + 1$  dimensionally unstable saddles embedded in higher-dimensional dynamical systems, where  $j$  is any positive integer; in a strange attractor, some of saddles could be vanished by SN bifurcations with a parameter perturbation.

### 3. Local attraction after SN bifurcation

Before introducing an idea to suppress an SN bifurcation, let us consider an example of such a bifurcation in the Duffing equations [Guckenheimer & Holmes , 1983; Thompson & Stewart , 1986] as follows:

$$\frac{dx}{dt} = y, \quad \frac{dy}{dt} = ky - x^3 + B_0 + B \cos t, \quad (4)$$

where  $k$ ,  $B_0$  and  $B$  are the parameters. We set  $k = 0.2$ ,  $B_0 = 0.27$  and  $B = 0.28$  nominally, then there exist three periodic solutions (see Fig. 1) [Kawakami , 1984]. The large and small periodic orbits are stable, and middle one is one-dimensionally unstable. Represent the solution as  $\mathbf{x}(t) = \boldsymbol{\varphi}(t, \mathbf{x}_0)$ , where  $\mathbf{x}(0) = \boldsymbol{\varphi}(0, \mathbf{x}_0) = \mathbf{x}_0$ . By taking the Poincaré map  $T: \mathbf{x}(t) \mapsto \mathbf{x}(t + 2\pi) = \boldsymbol{\varphi}(t + 2\pi, \mathbf{x}_0)$ , a periodic solution with period  $2\pi$  is converted into a fixed point;  $S_1$  and  $S_2$  are stable fixed points, and  $D$  is a saddle-type fixed point. They are connected through an unstable manifold  $W^u$  of  $D$  (see the red line in Fig. 1). The stable manifold  $W^s$  of  $D$  splits the state space into basins of attraction for  $S_1$  and  $S_2$  (the blue line in

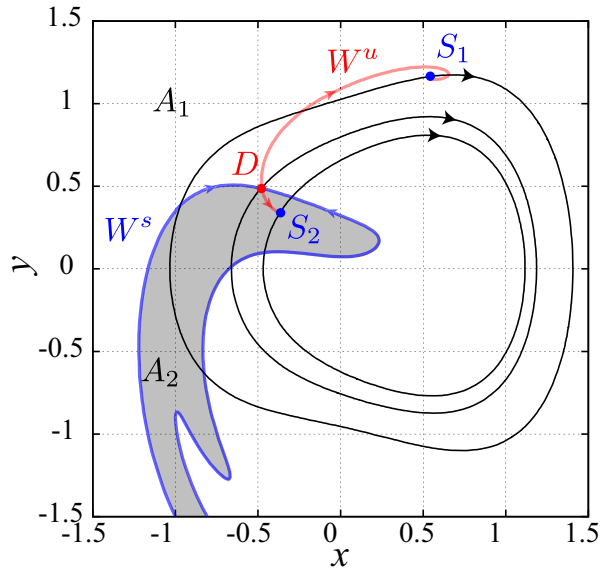


Fig. 1. Phase portrait of Eqs. (4) with  $k = 0.2$ ,  $B_0 = 0.27$  and  $B = 0.28$ .

Fig.1); the shaded region  $A_2$  is the basin of attraction for  $S_2$ . The process of an SN bifurcation is shown in Fig. 2. As we increase the parameter  $B_0$ , the inner two fixed points  $S_2$  and  $D$  gradually approach each other and eventually vanish at an SN bifurcation point with  $B_0 = B_0^* \approx 0.27853$ , and  $\mathbf{x}^*(0) = (-0.425, 0.413)$ . Accordingly, the basin of attraction  $A_2$  is cleared away, and the whole state space belongs to the basin of  $A_1$  (see Fig. 2(c)).

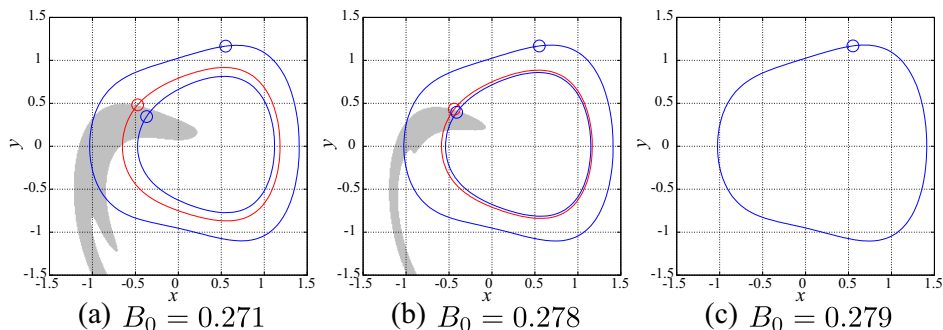


Fig. 2. Phase portraits before and after an SN bifurcation ( $k = 0.2$  and  $B = 0.28$ ).

Right after the SN bifurcation, even though a couple of periodic orbits have disappeared, a certain trajectory stays comparatively longer around the point corresponding to the coalescence of  $D$  and  $S_2$  which existed before the SN bifurcation. For example, Fig. 3 shows that a trajectory starting from an appropriate initial point takes many turns around the periodic orbit corresponding to  $S_2$  which existed before the bifurcation, then it finally converges to a periodic orbit corresponding to  $S_1$ . Hereafter, we call this solution an attractor ruin [Kaneko & Tsuda, 2003], that might be related to a slow perpetual point [Prasad, 2015].

Figure 4 depicts the transient time of each initial point  $\mathbf{x}_0$  in the state space with  $B_0 = 0.28$ . The gray scale expresses how long the orbit spends before converging into  $S_1$ . We notice that the darker area looks like the basin of attraction shown in Fig. 2 (b). Though all orbits go  $S_1$  asymptotically, the distribution of the transient time is uneven in the state space, i.e., orbits starting from the darker area spend more time before the convergence.

Let  $P$  be a point which location is where  $S_2$  and  $D$  coalesced together at  $B_0 = B_0^*$ . Consider the orbit

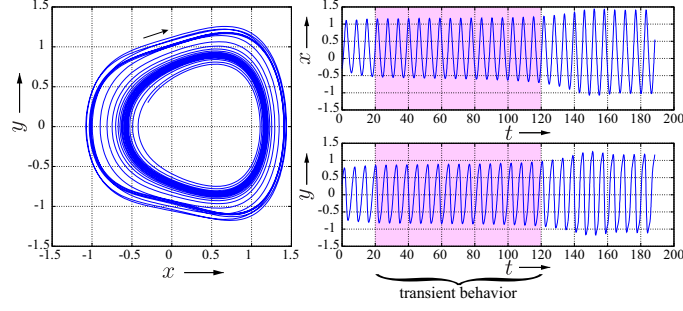


Fig. 3. Trajectory after the SN bifurcation, where  $k = 0.2$ ,  $B_0 = B = 0.28$ , and  $\mathbf{x}(0) = (-0.3, 0.3)$ .

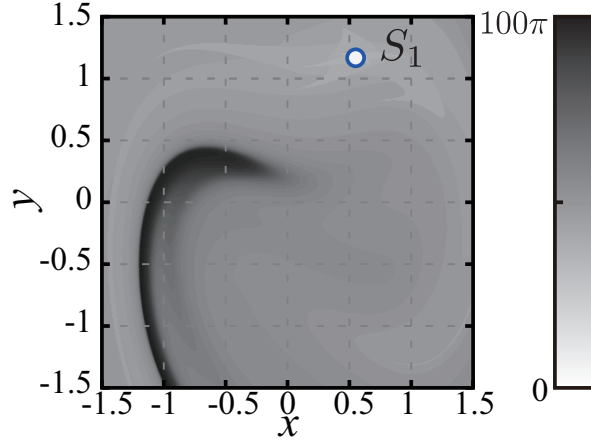


Fig. 4. Transient time before converging to  $S_1$ , starting from different initial conditions in the state space.

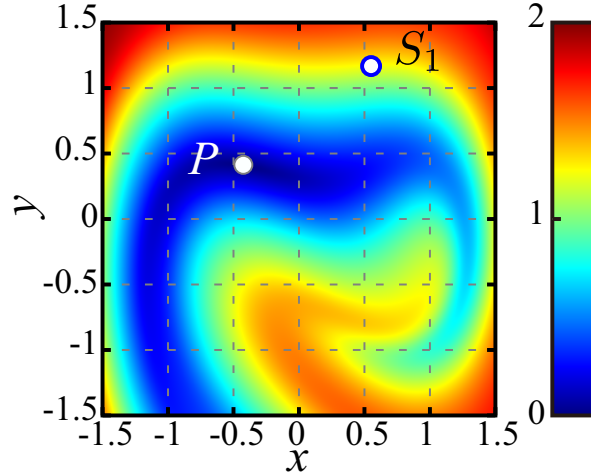


Fig. 5. Minimum distance between mapped points of  $T$  and  $P$ , that characterizes temporary attraction for the attractor ruin  $P$ , after the SN bifurcation with  $k = 0.2$ , and  $B_0 = B = 0.28$ .

starting from  $P$  for one cycle  $2\pi$  of the force  $B \cos t$  in Eqs. (4);  $\mathbf{x}(t) = \varphi(t, P)$ ,  $0 < t < 2\pi$ . It does not form a periodic orbit, but  $\varphi(2\pi, P)$  is close to  $\varphi(0, P)$ . We define a pseudo periodic orbit (PPO)  $\hat{\mathbf{x}}(t)$  according to the attractor ruin by bridging the gap with a tiny impulse  $\mathbf{q}$  such that  $\varphi(2\pi + 0, P) = \varphi(2\pi - 0, P) + \mathbf{q}$ , where  $\mathbf{q} = \varphi(0, P) - \varphi(2\pi - 0, P)$ . The fixed point of the PPO  $\hat{\mathbf{x}}(t)$  is  $P$ .

Figure 5 visualizes  $\min \|P - \varphi(2\pi k, \mathbf{x}_0)\|$  subject to  $k = 0, 1, \dots, 200$ , for each initial state  $\mathbf{x}_0$  in the

state space. The orbit starting from the blue area visits  $\hat{\boldsymbol{x}}(t)$  closely for some time during  $0 < t < 400\pi$ , and this area entirely covers the darker area in Fig. 4. From Figs. 3, 4, and 5, it is approximately ensured that the orbit starting from the darker area in Fig. 4 stays near  $\hat{\boldsymbol{x}}(t)$  for a comparatively long time. In other words, there exists a certain temporary basin of attraction for PPO  $\hat{\boldsymbol{x}}(t)$  even after the SN bifurcation.

#### 4. Catastrophe suppression control

Since not a few orbits autonomously visit areas near the PPO  $\hat{\boldsymbol{x}}(t)$  without any control input, this property can be used for preventing catastrophic transitions after SN bifurcations. Moreover, since such orbits approaches  $\hat{\boldsymbol{x}}(t)$  transiently, there is a possibility that a small control input might stabilize  $\hat{\boldsymbol{x}}(t)$ . Thus, a controller utilizing both of the features above should be able to suppress the catastrophic transition just after an SN bifurcation by using only a small amount of control energy.

The conventional methods of suppressing bifurcations are applicable to period-doubling bifurcations [Fang , 1993; Romeiras *et al.* , 1992] and Neimark-Sacker bifurcations [Ueta & Kawakami , 1995] since existence of UPOs are guaranteed after these bifurcations. The conventional methods rely entirely on this existence of the fixed points according to the UPO.

Now let us show how an SN bifurcation is virtually suppressed. If mapped points by  $T$  approach closely enough to  $P$ , i.e.,

$$\|P - \varphi(2\pi j, \boldsymbol{x}_0)\| < \epsilon, \quad (5)$$

is satisfied for some  $j$  and  $\epsilon$  with  $0 \leq \epsilon \ll 1$ , the control input

$$\boldsymbol{u}(t) = K(\boldsymbol{x}(t) - \hat{\boldsymbol{x}}(t)) \quad (6)$$

is applied to the system such that  $d\boldsymbol{x}/dt = \boldsymbol{f}(t, \boldsymbol{x}) + \boldsymbol{u}(t)$ . The checking mechanism for the inequality (5) is referred as a watcher. Through this control, the periodic orbit corresponding to  $P$ , which had disappeared once by the SN bifurcation, is restored and stabilized with suitable choice of  $K$ . Note that this control scheme does not affect other coexisting attractors.

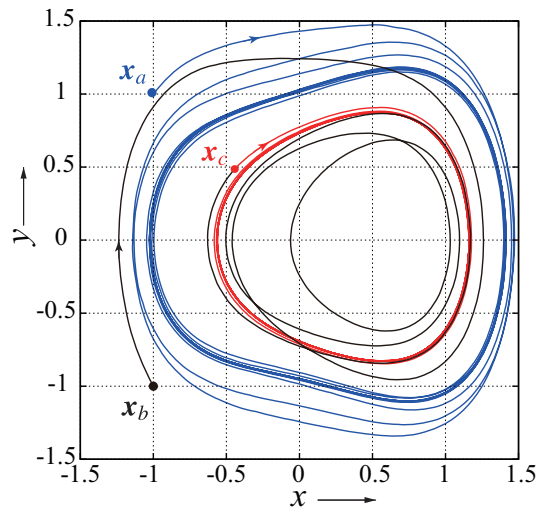


Fig. 6. Suppression of the SN bifurcation with  $\epsilon = 0.1$ . For the trajectory starting from  $\boldsymbol{x}_b$ , the control is not applied until arriving at  $\boldsymbol{x}_c$ .

Figure 6 shows the control response. We choose  $K = \kappa I$ , where  $\kappa = 0.3$ , and  $I$  is the  $2 \times 2$  identity matrix. In Fig. 6, an initial point  $\boldsymbol{x}_a$  is out of the temporary basin of attraction for  $P$ , and the orbit monotonously converges to  $S_1$  without control. On the other hand, another orbit starting from  $\boldsymbol{x}_b$  is in the temporary basin of attraction for  $P$ . Even without the control, the orbit gradually and autonomously approaches  $\boldsymbol{x}_c$  near  $P$ . In fact, at  $\boldsymbol{x}_c$ , the inequality (5) is satisfied, then the watcher starts the control. The orbit immediately converges to  $\hat{\boldsymbol{x}}(t)$  corresponding to  $P$  with a small-amplitude control input. No effect

occurs for the large periodic orbit with  $S^1$ . Figure 7 shows the time response of the control input for the orbit starting from  $\mathbf{x}_b$  in Fig. 6. At  $t \approx 24$ , the orbit reaches  $\mathbf{x}_c$  and the control gets started. Although periodic ripples remain in the control input because  $\hat{\mathbf{x}}(t)$  does not actually exist, they are negligibly small. This method is an extension of EFC. Instead of the UPO  $\mathbf{x}^*(t)$ , we use the PPO  $\hat{\mathbf{x}}(t)$ .

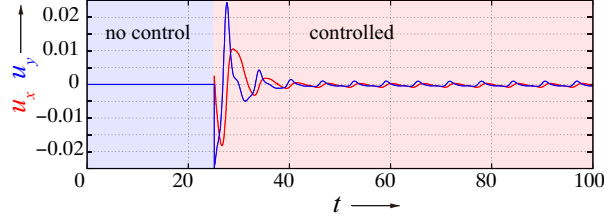


Fig. 7. Time response of the suppression control for the trajectory starting from  $\mathbf{x}_b$ .

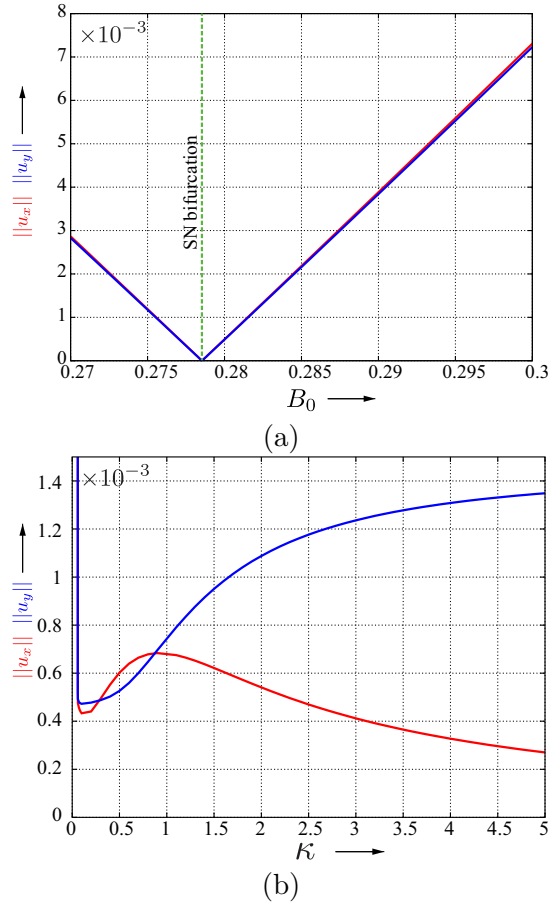


Fig. 8. Amplitudes of the control inputs. (a) Change of  $B_0$  with  $K = \kappa I$  and  $\kappa = 0.3$ . (b) Change of the control gain with  $B_0 = 0.28$ .

To show the robustness of this method, we will confirm the dependency on the parameters and the control gain. Figure 8(a) shows the variation in the control amplitude for  $B_0$  when we use the same PPO. Although the amplitude of ripples in  $\mathbf{u}(t)$  grow linearly as  $B_0$  increases from the bifurcation point, the PPO is well stabilized and the ripples are kept small. When we decrease  $B_0$  from the bifurcation point in Fig. 8(b), the original stable periodic orbit corresponding to  $S_2$  changes to the stable PPO with a small periodic control input. Figure 8(b) plots the amplitude of the control input as  $\kappa$  changes for  $B_0 = 0.28$ . Both  $u_x$  and  $u_y$  are restricted to be small with an appropriate choice of  $\kappa \in [0.2, 0.4]$ .

To illustrate the noise margin of the control, we add a white noise to the state when the control input is evaluated so that  $\mathbf{u}(t) = K(\mathbf{x}(t) + L\mathbf{n}(t) - \hat{\mathbf{x}}(t))$ , where  $\mathbf{n}(t) = (n_1(t), n_2(t))$  is a noise vector,  $n_j \in [0, 1]$ ,  $j = 1, 2$  is a uniform random number, and  $L$  is a parameter that shows the noise strength. Assume that  $\mathbf{n}(t)$  is updated every tick of the numerical integration. We use the Runge-Kutta method with a tick  $\Delta t = 0.01$ .

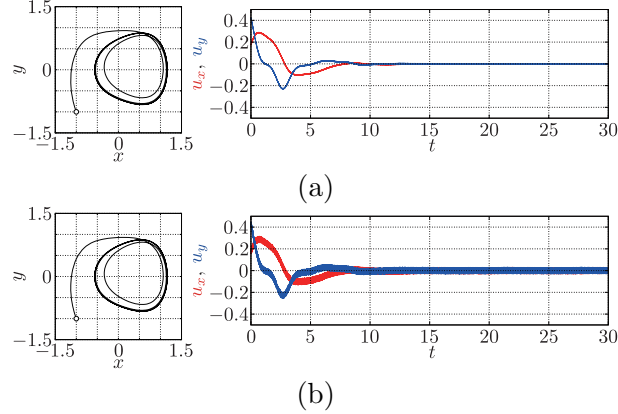


Fig. 9. Phase portraits and time responses for noisy control inputs with  $(x(0), y(0)) = (-1.0, -1.0)$ . (a):  $L = 10^{-2}$ , and (b):  $L = 10^{-1}$ .

Figure 9 shows time responses of control inputs with noisy state signals. The setup of the parameters and controller are the same as Fig. 6. We apply the control input from the initial point continuously. The figures show that the controlled state converges to  $\hat{\mathbf{x}}(t)$  even when the control input  $\mathbf{u}(t)$  contains small ripples.

Because the control input Eq. (6) is proportional to the difference between the current state and PPO, a large-amplitude control input might be generated if the controller is always switched on. Figure 10 shows full-time controlled trajectories starting from different initial points. These quick responses and global stability can be achieved if one admits such big-amplitude control inputs.

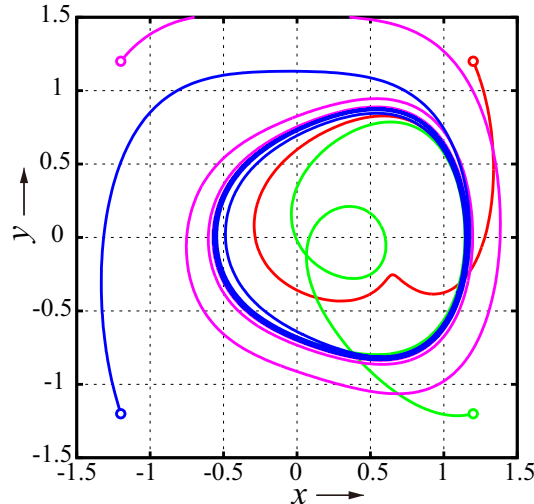


Fig. 10. Trajectories starting from different initial points. The control (6) is always activated with  $\kappa = 0.3$ .

## 5. Restoration of a limit cycle after an SN bifurcation

Our method is also applicable for autonomous systems. Here we demonstrate bifurcation suppressing control of a limit cycle in the Bonhöffer-van der Pol (BVP) oscillator [FitzHugh, 1961; Nagumo *et al.*

, 1962] both numerically and experimentally. With appropriate setting for the BVP oscillator, we have normalized equations as follows [Ueta *et al.*, 2004]:

$$\frac{dx}{dt} = -y + \tanh \gamma x, \quad \frac{dy}{dt} = x - \sigma y. \quad (7)$$

Assume that  $\gamma \approx 1.665$ . Around  $\sigma = 0.828$ , there are stable and unstable limit cycles, and they approach each other and meet at an SN bifurcation as  $\sigma$  increases further. Figure 11 shows the phase portrait just before the SN bifurcation. Note that the corresponding parameters are  $L = 50$ [mH],  $C = 0.1$  [ $\mu$ F],  $R = 4.7$  [k $\Omega$ ].

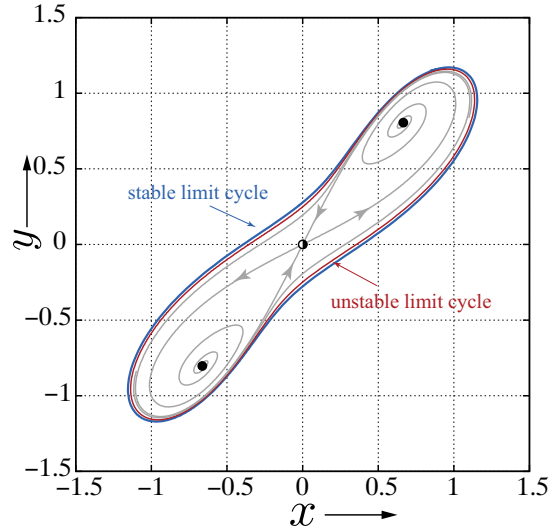
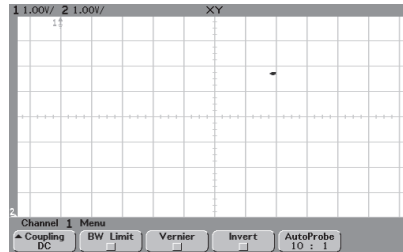
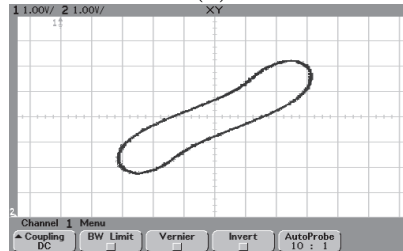


Fig. 11. Limit cycles just before their saddle-node bifurcation in the BVP oscillator.



(a)



(b)

Fig. 12. A restoration control of the limit cycle with  $\gamma = 0.8286$  in the laboratory experiment. The horizontal and vertical axes: 1 [V/div]. (a) Just after the SN bifurcation of limit cycles, we have a stable equilibrium point. (b) The controller (6) restores the limit cycle.

At  $\sigma = 0.8286$ , no limit cycle survives, and the orbits starting from almost all the initial points will be eventually absorbed into one of sink equilibria. However, orbits starting from large initial values wander

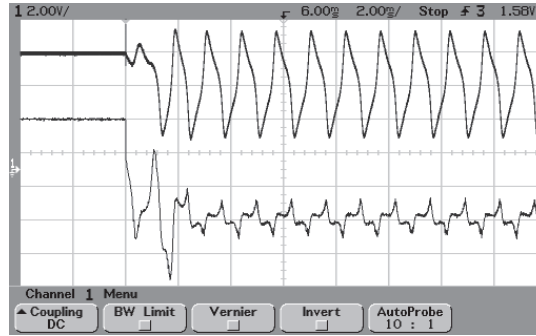


Fig. 13. Time responses of the control. The horizontal axis: 2 [msec/DIV]. Upper: Capacitor voltage corresponding to  $x$  in Eqs. (7) with the vertical axis: 2[V/div]. Lower: Injection current corresponding to the control input with the vertical axis: 0.2 [mA/div].

around the attractor ruin of limit cycles many times like Fig.3. Although the PPO can be applied as in the previous section, here we try to define another type of a simpler PPO for this problem as a variation more appropriate for laboratory experiments. We recorded one-cycle time series of  $\boldsymbol{x}(t)$  of the stable limit cycle at  $\sigma = 0.8285$  (before the bifurcation) as a PPO. If we apply Eq. (6) with this PPO to the system at  $\sigma = 0.8286$  (after the bifurcation), it is expected that the limit cycle can be restored by a small control input. We provide a control gain in Eq. (6) as

$$K = \begin{pmatrix} \kappa_{11} & 0 \\ 0 & 0 \end{pmatrix},$$

that is, the control input refers only the state  $x$  with  $x \in \boldsymbol{R}$ .

In the laboratory experiment, we used the controller by a LPC4088 (NXP semiconductors) to compute the difference between the voltage measured in real-time and the time series of the PPO stored in the memory, where the sampling rate is 50 [kHz]. We chose a control gain  $\kappa_{11} = 0.071$  corresponding to a 10 [k $\Omega$ ] resistor, and control input is realized as a current-injection source. Figure 12(b) shows a restored limit cycle with physical parameters according to  $\sigma = 0.8286$  where there is no limit cycle without any control. Figure 13 shows time series data of the restored limit cycle and the control input. Thereby we have demonstrated that a tiny periodic input restores a limit cycle at the parameter value where the system does not possess any limit cycle. In this experiment, we did not care about the watcher which should be used to detect sufficient approach of the trajectory to the target PPO because there is no another stable attractor in the controlled system.

## 6. Conclusion

We have proposed a resilient control scheme to suppress SN bifurcations. If the PPO information is provided adequately, a periodic orbit remains almost the same with a tiny control input even if the system meets an SN bifurcation. Both numerical and experimental results demonstrated robustness of the method. Since SN bifurcations are deeply related to the intermittent chaos, suppression of the chaotic bursting behavior by this method is a possible application.

## Acknowledgments

This research is partly supported by CREST, JST, and JSPS KAKENHI 25420373 and 15H05707.

## References

- Celka, P. [1994] "Experimental verification of Pyragas's chaos control method applied to Chua's circuit," *Int. J. Bifurcation and Chaos* 4(6), 1703–1706.
- Chen, G.(ed) [1999] *Controlling Chaos and Bifurcations in Engineering Systems*, (CRC Press, Boca Raton).

- Chen, G. & Dong, X. [1993] “On feedback control of chaotic continuous-time systems,” *IEEE Trans. CAS-I* **40**(9), 591–601.
- Chen, G., Hill, D. J. & Yu, X. (eds.) [2003] *Bifurcation Control: Theory and Application*, LNCIS 293 (Springer-Verlag, Berlin).
- Chen, L., Liu, R., Liu, Z.-P., Li, M. & Aihara, K. [2012] “Detecting early-warning signals for sudden deterioration of complex diseases by dynamical network biomarkers,” *Scientific Reports* **2**, 342–1–8.
- Christini, D. J. & Collins, J. [1996] “Using chaos control and tracking to suppress a pathological nonchaotic rhythm in a cardiac model,” *Phys. Rev. E* **53**(1), 49–52.
- Diakonou, F. K., Schmelcher, P. & Biham, O. [1998] “Systematic computation of the least unstable periodic orbits in chaotic attractors,” *Phys. Rev. Lett.* **81**(20), 4349–4352.
- Fang, H. [1993] “Suppression of period doubling in coupled nonlinear systems,” *Phys. Lett. A* **183**(5-6), 376–378.
- FitzHugh, R. [1961] “Impulses and physiological states in theoretical models of nerve membrane,” *Biophys J.* **1**(6), 445–466.
- Guckenheimer, H. & Holmes, P. [1983] *Nonlinear Oscillations, Dynamical Systems, and Bifurcations of Vector Fields* (Springer-Verlag, New York) Applied Mathematical Sciences **42**.
- Kaneko, K. & Tsuda, I [2003] “Chaotic itinerancy,” *Chaos* **13**(3), 926–936.
- Kawakami, H. [1984] “Bifurcation of periodic responses in forced dynamic nonlinear circuits: computation of bifurcation values of the system parameters,” *IEEE Trans. CAS-31*(3), 248–260.
- Nagumo, J., Arimoto, S. & Yoshizawa, S. [1962] “An active pulse transmission line simulating nerve axon,” *Proc. IRE* **50**, 2061–2070.
- Ogorzalek, M. [1993] “Taming Chaos: Part II—Control,” *IEEE Trans. Circuits and Syst. I* **40**(10), 700–706.
- Ott, E., Grebogi, C. & Yorke, J.A. [1990] “Controlling chaos,” *Phys. Rev. Lett.* **64**, 1196–1199.
- Prasad, A. [2015] “Existence of perpetual points in nonlinear dynamical systems and its applications,” *Int. J. Bifurcation and Chaos* **25**(2), 1530005–1–10.
- Pyragas, K. [1992] “Continuous control of chaos by self-controlling feedback,” *Phys. Lett. A* **170**(6), 421–428.
- Pyragas, K. [2006] “Delayed feedback control of chaos,” *Philos. Trans. A. Math. Phys. Eng. Sci.* **364**(1846), 2309–2334.
- Romeiras, F. J., Grebogi, C., Ott, E. & Dayawansa, W. P. [1992] “Controlling chaotic dynamical systems,” *Physica D* **58**, 165–192.
- Scheffer, M. [2009] *Critical Transitions in Nature and Society* (Princeton University Press, Princeton).
- Scheffer, M., Bascompte, J., Brock, W. A., Brovkin, V., Carpenter, S. R., Dakos, V., Held, H., van Nes, E. H., Rietkerk, M. & Sugihara, G. [2009] “Early-warning signals for critical transitions,” *Nature* **461**(7260), 53–59.
- Thompson, J.M.T. & Stewart, H.B. [1986] *Nonlinear Dynamics and Chaos: Geometrical Methods for Engineers and Scientists* (John Wiley & Sons Ltd., Chchester and New York).
- Ueta, T. Chen, G. & Kawabe, T. [2000] “A simple approach to calculation and control of unstable periodic orbits in chaotic piecewise linear systems,” *Int. J. Bifurcation and Chaos* **11**(1), 215–224.
- Ueta, T. & Kawakami, H. [1995] “Composite dynamical system for controlling chaos,” *IEICE Trans. EA* **78**(6), 708–714.
- Ueta, T., Miyazaki, H., Kousaka, T. & Kawakami, H. [2004] “Bifurcation of coupled BVP oscillators,” *Int. J. of Bifurcation and Chaos*, **14**, 4, pp.1305–1324.